Research Article Adv. Mater. Lett. 2015, **6**(9), 803-809 Advanced Materials *Letters*

www.amlett.com, www.vbripress.com/aml, DOI: 10.5185/amlett.2015.5915

Poly(o-anisidine) carbon fiber based composites as an introductory material for EMI shielding

Rakesh Kumar[1,2,3], Seema Joon[1,3], Avanish P. Singh[1], Brij P. Singh[2], S. K. Dhawan[1*]

[1]*Polymeric & Soft Material Section, CSIR-National Physical Laboratory, New Delhi 110012, India*
[2]*Department of Chemistry, DCRUST Murthal, Sonipat, Haryana 130001, India*
[3]*PDM College of Engineering, Bahadurgarh, Haryana 124507, India*

[*]Corresponding author. Tel: (+91)1145609401; E-mail: skdhawan@mail.nplindia.ernet.in

Received: 03 February 2015, Revised: 30 April 2015 and Accepted: 08 May 2015

ABSTRACT

In response to the striking research activity and publications in fabrication of multifunctional materials, the present work is an attempt to fabricate processible composite sheets of poly (o-anisidine)-carbon fiber (PoACF) by a facile, low cost method and find their use in electromagnetic interference (EMI) shielding in X-band (8.2-12.4 GHz). PoACF composite is synthesized by *in-Situ* oxidative emulsion polymerization and transformed into thin sheets by compression molding technique using different ratio of phenolic novolac resin as a binder. The prepared PoACF composites and sheets are characterized by SEM, TGA, UV-vis, & FT-IR techniques. PoACF sheets have conductivity of the order of 10^{-3} to 10^{-1} S/cm and maximum shielding effectiveness of 32.57 dB at 4 mm thickness. These sheets have flexural strength between 18.82 to 41.28 MPa. The sheets of PoACF composite have sufficient thermal as well as mechanical stability and may be accepted as an economical material for EMI shielding application.

Keywords: PoACF thin sheets; carbon fiber; mechanical properties; electrical properties; EMI shielding.

Introduction

A detailed introduction is required here with proper emphasis about: (i) Importance of the addressed subject in general, (ii) importance of addressed subject in particular, (iii) related aspects covered in the literature, (iv) at the end a clear motivation about what is uniqueness about the present work (what is new here or how it differs from the previous works). It must be written in such a way that readers can get a detailed overview about the addressed subject (past, present and future perspectives and challenges). References should be listed as: [**1**] wherever needed.

Intrinsically conducting polymers (ICPs) like polyaniline, polypyrrole, polythiophene, etc. have attracted much attention in most recent times as a result of their potential application in many technological areas such as sensors [**1**], rechargeable batteries **[2]**, molecular electronic devices [**3**], smart windows [**4**], electrochromic displays [**5**], energy storage systems [**6, 7**]. One of the most important and promising applications of ICPs is as EMI shielding [**8, 9**] material to minimize electromagnetic pollution. With the development in the field of electronics and communication, electromagnetic pollution has become a major problem in most of the developed and developing countries. Materials made by ICPs like, fiber/CNT/ nanowires/nanomaterial filled polymer composites [**10-12**], segregated ICP composites [**13, 14**] and conducting polymer blends [**15**] have reached up to their commercial level for their application in EMI shielding. Still there are scopes to use these materials at large scale to make durable and hard as well as flexible enclosures for electronic equipments for protection against electromagnetic radiations.

Among the class of conducting polymers, polyaniline (PANI) is the most promising polymer for EMI shielding and other potential applications because of its excellent environmental stability in combination with relatively high conductivity [**16**]. However, this polymer with most of other conducting polymers suffers from poor processibility, poor solubility and infusibility due to the stiffness of its backbone. In this regard, efforts have been made to synthesize functionalized polymers, copolymers and conducting polymeric composite materials [**17-19**]. Derivatization is one of the trendy methods to improve the flexibility and thereby the processibility of PANI chains [**20-22**]. Various reports have suggested that derivatives of PANI exhibit low conductivity and have been utilized only for applications that rely on low conductivity such as sensors, corrosion inhibitors [**23-26**]. Our previous report on thin sheets of polyaniline-carbon fiber-novolac composites [**27**] inspired us to search new composites of suitable PANI derivative and apply them for EMI shielding application. To the best of our knowledge we are reporting here first time, the synthesis and application of poly (o-anisidine)-carbon fiber (PoACF) composite, for EMI shielding applications. Desired conductivity for this purpose have been achieved by incorporation of carbon fiber (CF) as conducting filler into poly (o-anisidine) (PoA) matrix during polymerization process. PoACF composite so prepared were molded into the form of thin sheets by compression molding technique using phenolic novolac resin (PNR) as binder. Here, in this work the amount of CF into PoACF composite is fixed (20% by wt. of monomer) as this much amount of CF is sufficient to achieve the desired value of conductivity for EMI shielding application [**27-30**], but another parameter, i.e. loading of PNR into PoACF composite was varied to optimize the thermal, mechanical, electrical and shielding properties of the sheets. The prepared sheets of PoACF, due to their unique combination of hardness and flexibility have potential to be used as durable enclosures for electronic devices.

Experimental

Materials

Ortho-anisidine (o-methoxy aniline) from Merck, India was freshly distilled before use. Reagent-grade sodium lauryl sulphate (SLS, Himedia, India), ammonium persaulfate (APS, Merck, India) and hydrochloric acid (Merck, India) were used as received. Polyacrylonitrile (PAN) based carbon fibers (CF, Toray-T-300-Japan) were chopped to get fiber size of 5-6 mm prior to use. Phenolic novolac resin (PNR, Pheno-organic, India) was used as binder for making sheets of PoACF composites.

In-Situ synthesis of PoACF composite

PoACF composite was synthesized by in-*Situ* chemical oxidative emulsion polymerization. Firstly, 0.1M SLS was dissolved in distilled water and homogenized for half an hour, then 0.1 M HCl was added to this aqueous solution of SLS to maintain a pH of 2-3. Further, this acidified aqueous solution of SLS so converted to form dodecyl hydrogen sulphate (DHS), was homogenized for 1 h with the addition of chopped CF (20% by wt. of monomer, anisidine) of 5 mm average length. 0.1M anisidine was then added to the above solution and homogenized again for 1 h to form micelles (emulsion) of anisidine-CF with DHS. This emulsion of anisidine and DHS was transferred to the reactor and polymerized at -3°C through chemical oxidative polymerization by drop wise addition of 0.1 M APS and continuous stirring for 6-7 h. The polymer composite so prepared was filtered, washed & then dried at ~ 70°C in vacuum oven. Finally it was crushed to get PoACF composite powder. In this composite PoA acts as a conducting polymer matrix and CF as a conducting filler which improves the electrical as well as mechanical and thermal properties of the composite material. Here, in this synthesis DHS acts as surfactant as well as dopant. By the similar route, pristine PoA doped with DHS was also synthesized for comparative study.

Fabrication of thin sheets of PoACF composite

Thin sheets (thickness ~ 0.8 mm) of PoACF composites were prepared by compression moulding technique using PNR as a binder. The PoACF composite powder was mixed and grinded (2h, 300rpm) with PNR powder in different ratios (5, 15, & 25 wt. % of PoACF) using Retsch "PM-400" planetary-ball mill in tungsten carbide jars. These samples were then dispersed in ethanol (10% by wt. of mixture) by means of ultrasonication for 2-3 h. Ethanol was then evaporated at ~ 50°C temperature and the samples were again dried at ~ 70°C. Thin sheets of these powdered samples were prepared by compression moulding technique at 100°C temperature and contact pressure. These sheets were further cured in the mold at 150°C temperature for 2h. Before ejecting the sheets from the mould, post curing was carried out by thermal annealing of the sheets from 150°C to room temperature, which took about 4h. The PoACF composite sheets so obtained were abbreviated as PoACF5 (5 wt. % of PNR), PoACF15 (15 wt. % of PNR) and PoACF25 (25 wt. % of PNR).

Materials Characterization

The morphology of PoACF composite samples were examined by scanning electron microscope (SEM, Zeiss EVO MA-10). Thermal stability of the samples was done by thermo gravimetric analyzer (Mettler Toledo TGA/SDTA 851^e) under inert atmosphere (flowing N_2 gas) in the temperature range of 25-900°C, at a uniform heating rate of 8°C/min. UV-vis absorption studies were carried out on Shimadzu 1601 spectrophotometer in the wavelength range of 200-1100nm. Fourier transform infrared (FTIR) spectra were recorded on Nicolet 5700 in the wavenumber range of 3500-500cm^{-1}. Flexural strength of composite sheets was measured by Instron universal testing machine (model 4411). Room temperature conductivity of the PoACF composite and PoACF sheet samples was measured by a standard four-probe technique using Keithley programmable current source (model 6221). Electromagnetic shielding measurements of PoACF sheets, cut with dimensions of 25.7×13mm, were carried out using Agilent E8362B Vector Network Analyzer in the frequency range of 8.2-12.4 GHz (X band of microwave region). To increase the thickness, multiple sheets were inserted in the cavity present in copper sample holder (see supporting information) and connected between the waveguide flanges of Network Analyzer.

Results and discussion

Fig. 1 depicts the SEM images of PoA, PoACF & PoACF15 composite powder and high resolution optical image of PoACF25 sheet sample. From the micrographs (**Fig. 1a**), it is observed that PoA exist in globular morphology. The observed globular structure of PoA (due to DHS used as surfactant) is similar to the previous reports given for PANi doped with DHS [**27, 31**]. It has been reported that morphology of the microstructure depends on preparation conditions as well as on the structure & concentration of dopant and oxidant. **Fig. 1(b)** displays the insertion and distribution of CF into the PoA matrix. It also shows the heterogeneous coating of globular PoA molecules on the surface of CF indicating that CF were well dispersed and immersed in the polymer matrix. PoACF composite shows new interwoven fibrous structure, which act as conductive pathway and lead to enhanced conductivity than that of pure PoA. *In-situ* oxidative emulsion polymerization of PoA along with CF facilitate the CF to be surrounded by globular PoA molecules which lead to the formation of multiparticle clusters and conducting channels in the composite [**32**]. **Fig. 1(c)** (micrograph of PoACF15 composite) shows that PNR used as binder in the composite created a strong fiber-matrix interfacial interaction which led to the formation of much compact structure of composite. Due to increase in fiber-matrix interaction, the connectivity of fibers with each other and also with the polymer matrix increases and there is formation of highly dense conducting network which defend the conductivity of PoACF and does not allow the insulating PNR to decrease the conductivity of the composite significantly, but upto low loading of resin. This fiber-matrix interaction further increases upon compression moulding of the composite to get PoACF sheets. **Fig. 1d** displays the high resolution optical image of fabricated PoACF25 sheet.

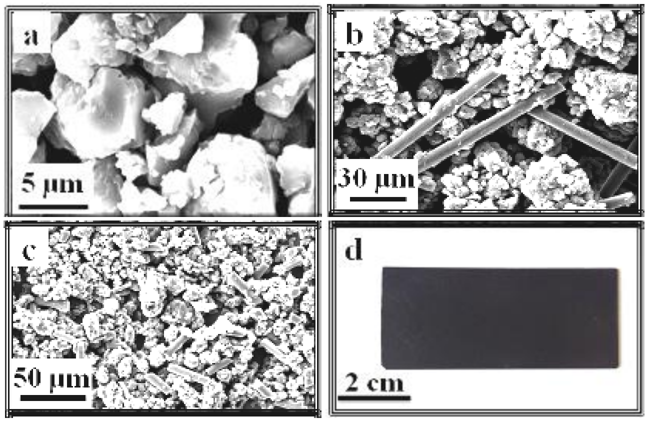

Fig. 1. SEM images of (a) PoA, (b) PoACF and (c) PoACF15 composite powder and (d) High resolution optical image of PoACF25 sheet.

UV-Vis spectroscopy (**Fig. 2a**) gives information regarding the doping of PoA with DHS. The DHS doped PoA shows absorption peaks at 342nm, 428nm and 866nm. The peak at 342nm corresponds to π-π* electronic transition of the benzenoid rings; the peak at 428 nm corresponds to partial oxidation of PoA and can be assigned to the localized polarons which are the characteristic of protonated PoA. This peak represents the intermediate state between leucoemaraldine form having benzenoid rings and emaraldine form having conjugated quinoid rings in the backbone of the PoA. The peak at 866 nm (bipolaron) is assigned for the transformation of emaraldine form of PoA to fully oxidized pernigraniline form. This confirms that the polymer is composed of different conducting phases and PoA polymer is doped with DHS as high as bipolarons are formed. Comparison of UV-Vis spectra of PoA with the spectra of PoACF and PoACF5 (**Fig. 2a**) displayed that there is no significant change in the position of peaks except a slight blue shifting in second and third peak.

FTIR spectroscopy is one of the most valuable tools for structural elucidation of molecules / macro molecules. FTIR study of the composites has been carried out to confirm the synthesis of PoACF composite and to see the interaction of CF with PoA and PNR in the three phase system. **Fig. 2(b)** demonstrates the FTIR spectra of PoACF, PoACF5, PoACF15 & PoACF25 composites. Main characteristic peaks of PoA in PoACF composite appear as reported in the earlier reports of PoA doped with different sulphonic acids **[33, 34]**. Slight shifting in the position of peaks is due to the interaction of PoA with CF and PNR. In the FTIR spectrum of PoACF composite a broad & weak band at 3128 cm^{-1} is due to aromatic C-H stretching; the bands at 1571 & 1488 cm^{-1} are for C=N and C=C stretching modes of quinoid (Q) and benzoid (B) rings; bands at 1288 and 1010 cm^{-1} are assigned to the presence of an o-methoxy group in the structure of PoA; the band at 1207 cm^{-1} is considered as a measure of electron delocalization on PoA and is referred to as the electronic like band, which is a characteristic peak of PoA conductivity [**35**]; a band at 1120 cm^{-1} is attributed to C-H in plane bending vibration, which is formed during protonation, and a band at 806 cm^{-1} indicates the ortho- substituent on benzene ring. Besides these normal peaks of PoA, the bands at 2915 & 2846 cm^{-1} are due to asymmetric and symmetric aliphatic C-H stretching vibrations respectively [**36**], which indicates the presence of alkyl substituent of DHS in PoA chain.

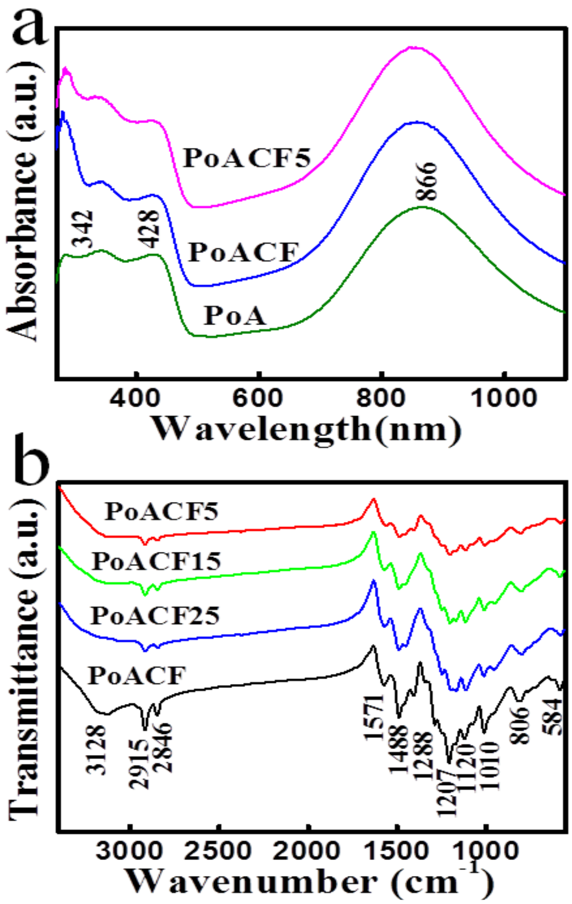

Fig. 2. (a) UV-vis spectra of PoA, PoACF and PoACF5 powder samples, (b) FTIR spectra of PoACF, PoACF5, PoACF15 & PoACF25 composites.

Further the presence of SO_3^- group of DHS (used as dopant as well as surfactant) is confirmed by the appearance of a band at 584 cm^{-1}, which is due to degenerate bending mode of SO_3^- group [**31**]. On comparing the spectra of PoACF composite with spectra of PoACF5, PoACF15 & PoACF25 composites (**Fig. 2b**) it is observed that, upon addition of PNR as binder into PoACF composite, there is no appearance of new band in the spectra of PoACF composites, which indicates that there is no net chemical reaction of PNR with PoA & CF. Here, PNR just act as a binder and have physical or some ionic interfacial interaction with PoACF composite. Absence of new covalent bonding between PNR and PoA/CF results in the same IR spectra except slight shifting in the position of some main peaks of PoACF, which is due to strong interfacial interaction of PNR with PoA chains & CF. The FTIR results so observed confirm the synthesis of PoACF composites.

TGA is carried out to evaluate the thermal stability of the composite sheets. **Fig. 3a** represents the thermogram of PoACF composite doped with DHS and PoACF sheets with different loading of PNR in PoACF composite. The thermal behavior of PoACF is similar to that of polyaniline [**33-37**], which exhibts a three step decomposition pattern. In first stage weight loss up to 110°C is due to the loss of water molecules/ moisture entrapped in the polymer matrix. The second stage weight loss observed from 110°C to 290°C is attributed to the removal of dopant (dedoping) from the polymer chains. The third stage loss from 290°C onwards is responsible for complete degradation and decomposition of the polymer backbone. On comparing the thermogram of PoACF composite with thermograms of PoACF sheets (**Fig. 3a**) it is found that thermal stability of the PoACF composite increases when it is transformed into the form of thin sheets by blending with PNR, which further increases with increase in the amount of PNR in the composite sheets. On comparison of thermograms of PoACF and PoACF 25 sheet, it is observed that in the first stage, 5.2 % weight loss occurs in case of PoACF, while only 1.4 % weight loss occurs in PoACF25 sheet, as the sheet was already thermally cured at 150°C. In case of PoACF25 sheet the second and third step is less conspicuous involving gradual weight loss extending over a broad range of temperature. Also in case of PoACF25 sheet 42% of the original weight is stable up to 900°C, which is more as compared to the case of PoACF (21% weight loss). This proves that PNR used as binder in sheet preparation of PoACF composite improved the thermal stability of polymer composite.

Table 1. Flexural strength, flexural modulus, electrical conductivity and shielding effectiveness of different samples

Sample name	Carbon fiber (wt. %)	Novolac resin (wt. %)	Flexural strength (MPa)	Flexural Modulus (GPa)	Electrical conductivity (S/cm)	Shielding effectiveness (dB) at 12.4 GHz	Thickness of sample (mm)
PoA	0	0	—	—	0.94×10^{-3}	—	—
PoACF	20	0	—	—	2.43×10^{-1}	—	—
PoACF5	20	5	18.82	0.09	0.95×10^{-1}	7.5	0.79
PoACF15	20	15	30.75	0.22	0.64×10^{-1}	8.8	0.82
PoACF25	20	25	41.28	0.34	0.28×10^{-2}	3.6	0.78

The electrical conductivity, flexural strength and shielding effectiveness of PoA, PoACF composite and PoACF sheets are tabulated in **Table 1**. The PoA & PoACF composite have conductivities of 0.94×10^{-3} S/cm and 2.43×10^{-1} S/cm respectively. As expected the conductivity increases by two orders with the addition of CF. As explained earlier and confirmed by the SEM micrographs of PoACF composite powder that the facile method of *in - Situ* oxidative polymerization of o-anisidine along with carbon fiber, these fibers are thought to be surrounded by globular o-anisidine molecules which lead to form multiparticle clusters and conducting channels in the composite sheet [**32**], so the conductivity increases by addition of carbon fiber in pristine PoA. When PoACF composite was blended with PNR in different ratios to get PoACF5, PoACF15 and PoACF25 composites, the conductivity decreases with increase in the wt. % of PNR (inset of **Fig. 3b**) in the composite, which is due to the insulating nature of resin. But when these composites are transformed into thin sheets by press moulding technique, the conductivity again increases (see supporting data). PNR being strong binder increases the wettability and dispersion of short carbon fiber in the polymer matrix and the interaction between carbon fibers and polymer matrix increases, thereby enhancing the connectivity of fillers and matrix. Moreover, during the moulding of the sheets the excess of PNR squeezed out after doing its action. In the present study amount of CF in the polymer matrix is although fixed (20% by wt.), but loading of PNR in PoACF composite is varied to optimize the mechanical, electrical and shielding properties in the PoACF sheets.

Mechanical strength of the sheets are explained in terms of measurement of flexural strength and flexural modulus by three point bending test based on ASTM D790 [**38**] using an Instron Universal Testing Machine (model 4411) at a crosshead speed of 0.5 mm/min. The specimens with a length of 70 mm, width 20 mm and thickness ~ 0.8 mm were taken to measure this three-point test. The support span length (L) between the two supports of specimen was 40 mm. **Table 1.** shows the values of flexural strength and flexural modulus of different sheet samples. It is found that flexural strength and flexural modulus increase considerably (**Fig. 3b**) with increase in the percentage of PNR in the composite sheets. PNR improves the interfacial interactions between resin and carbon fiber surface and hence the load is facilitated to be transferred between the resin and the fillers. PNR is a strong binder, so improves the adhesion bonding between the fillers and polymer matrix which provide higher strength by enabling the stress to be transferred around the stiff filler phase. Sheets become stiffer due to crosslinking of the resin during thermal curing of the sheets at 150°C.

In the present study effect of PNR on mechanical properties has been studied up to 25 wt. % loading of resin, as up to this limit the conductivity and shielding properties of PoACF sheets have been decreased extensively due to the insulating character of the resin. The electromagnetic interference is defined as spurious voltage and current induced in the electronic circuit by the external sources. The shielding effectiveness (SE) is a typical value that quantities the amount of attenuation in a specific material. If P_{in} is the incident power density at a measuring point before the shield is in place, P_{trans} is the transmitted power density at the same measuring point after the shield is in place, then [**39-41**]

$$SE\ (dB) = -10 \log (P_{trans}/P_{in}) \quad (1)$$

The measurement of EMI shielding effectiveness is basically an insertion loss expressed in decibels (dB). For a shielding material, total SE = $SE_R + SE_A + SE_M$, where SE_R, SE_A, and SE_M are shielding effectiveness due to reflection, absorption, and multiple reflections, respectively. In two port network, S-parameters S_{11} (S_{22}), S_{12} (S_{21}) represents the reflection and the transmission coefficients given as,

$$R=|S_{11}|^2=|S_{22}|^2 \quad (2)$$

$$T=|S_{21}|^2=|S_{12}|^2 \quad (3)$$

And absorption coefficient; A=1-R-T

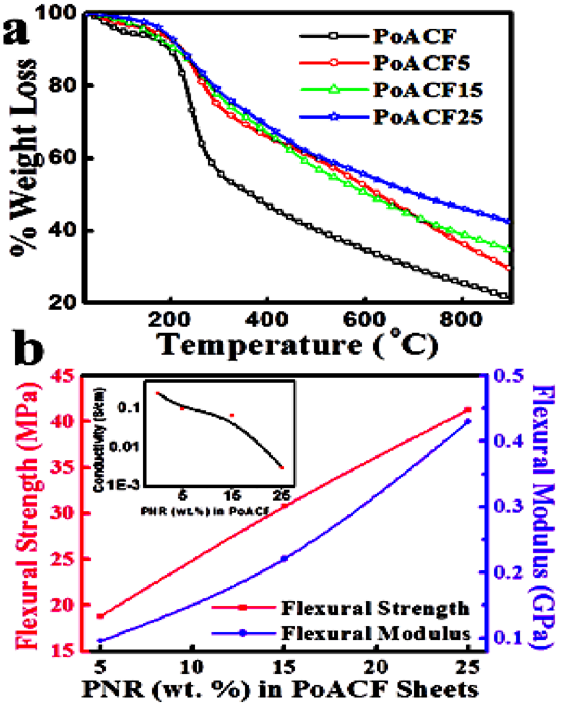

Fig. 3. (a) TGA of PoACF composite powder, PoACF5, PoACF15 & PoACF25 sheets, (b) Variation of flexural strength and flexural modulus as a function of wt. % of PNR in PoACF sheets. Inset of (b) Variation of conductivity as a function of wt.% of PNR in PoACF sheets

Here, absorption coefficient is given with respect to the power of the incident electromagnetic wave. If the effect of multiple reflections between both interfaces of the material is negligible, then the relative intensity of the effectively incident electromagnetic wave inside the material after reflection is based on the quantity (1- R). Therefore, the effective absorbance (A_{eff}) can be described as $A_{eff} = (1 - R - T) / (1 - R)$ with respect to the power of the effective incident electromagnetic wave inside the shielding material. It is convenient to express the reflectance and effective absorbance in the form of $-10 \log (1 - R)$ and $-10 \log (1 - A_{eff})$ in decibel (dB), respectively, which give SE_R and SE_A as,

$$SE_R = -10\log(1-R) \quad (4)$$

$$SE_A = -10\log(1-A_{eff}) = -10\log(T/1-R) \quad (5)$$

The SE of PoACF sheets containing different concentration of PNR (5, 15, 25 wt. %) have been measured in the X-band frequency range. **Fig. 4a** shows the variation of SE_R & SE_A of these sheets in 8.2-12.4 GHz frequency range which depicts that both SE_R & SE_A contributes to total SE. Though, the contribution of SE_A is more than SE_R as reported in previous studies **[42, 43]**. The value of SE_T for PoACF5, PoACF15, PoACF25 are 3.6, 7.5 and 8.8 dB respectively, at a matching thickness of ~ 0.8 mm at 12.4 GHz. From this it is concluded that the SE first increases with the increase in the loading of PNR from 5 to 15 wt. %, then it decreases at 25 wt. %. Thus SE is found to be maximum for POACF15 sheet that may be probably due to the presence of PNR which is acting as binder thereby, creating a strong fiber-matrix interface interaction that enhances the connectivity and so the shielding effectiveness. At the same time the insulating behavior of resin dominates at 25 wt. % loading of PNR that result in the decrease of SE.

Fig. 4b shows the variation of total SE of PoACF15 at different thickness (0.8–4.0 mm) (multiple sheets) with frequency. The graph indicates that the SE gradually increases with the increase in thickness. The composite sheets up to 3 mm thickness shows SE of 8 to 27dB while the SE value of 32.5 dB was observed at a thickness of 4 mm. It is noteworthy that, a SE value of 20-30dB is required for techno-commercial applications, it means a sheet of PoACF having thickness equal to or greater than 2.4 mm could be potentially used for EMI shielding.

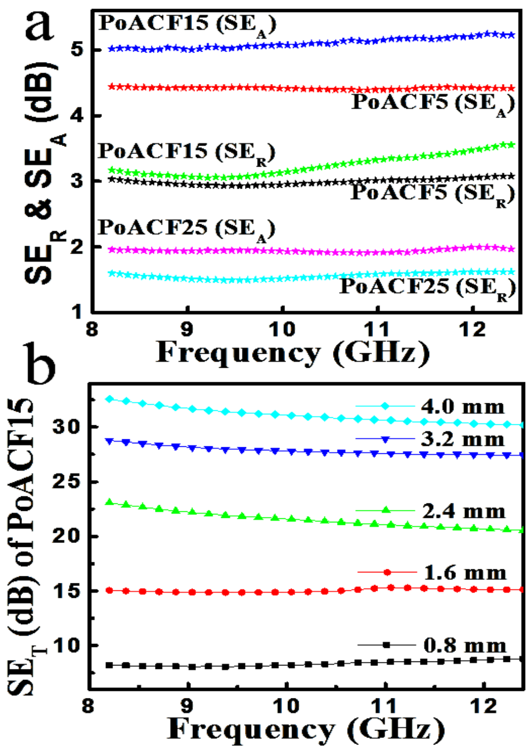

Fig. 4. (a) Variation of shielding effectiveness SE_A & SE_R with frequency in 8.2-12.4 GHz, showing effect of PNR concentration in PoACF sheets, (b) SE_T of PoACF15 sheets with different thickness.

PNR improves the interfacial interactions between resin and carbon fiber surface and hence the load is facilitated to be transferred between the resin and the fillers. PNR is a strong binder, so improves the adhesion bonding between the fillers and polymer matrix which provide higher strength by enabling the stress to be transferred around the stiff filler phase. Sheets become stiffer due to crosslinking of the resin during thermal curing of the sheets at 150°C. In the present study effect of PNR on mechanical properties has been studied up to 25 wt. % loading of resin, as up to this limit the conductivity and shielding properties of PoACF sheets have been decreased extensively due to the insulating character of the resin.

Conclusion

Using PNR as binder, PoACF sheets have been successfully prepared by compression moulding technique. The fabrication of these sheets is easy due to better processability of the composite because of the flexible PoA chains. Phenolic novolac resin & carbon fiber mutually boost the mechanical and thermal properties of PoACF sheets. Insertion of conducting filler in the poly (o-anisidine) matrix enhances the electrical & shielding properties of the sheets. By increasing the filler matrix interfacial attraction, PNR improves the mechanical and thermal properties of PoACF sheets without affecting the shielding properties significantly. It has been observed that flexural strength of PoACF sheets increases up to 41.28 MPa and flexural modulus up to 0.34 GPa. Thermal stability of PoACF sheets is ~ 210°C. Thin sheets of PoACF composite with 15% loading of PNR have maximum shielding effectiveness of 8.8 dB at 0.82mm thickness in 8.2-12.4 GHz frequency range. But PoACF sheets at higher thickness of 4.0mm (multiple sheets) have SE up to 32dB. The obtained data shows that PoACF sheets, due to their lightweight and ease of processing, can be used in techno-commercial applications for microwave shielding.

Acknowledgements

The authors wish to thank Director CSIR-NPL and Chairperson, Department of Chemistry, DCRUST for their keen interest in the work. The authors thank Dr. R.B. Mathur for the measurement of mechanical properties and K.N. Sood for recording SEM micrograph.

Reference

1. Sengupta, P. P.; Barik, S.; Adhikari, B. *Mat. and manufact. pro.* **2006,** *21*, 263. **DOI:** 10.1080/10426910500464602
2. Song, H. K.; Palmore, G. T. R. *Ad. Mat.* **2006,** *18*, 1764. **DOI:** 10.1002/adma.200600375
3. Saxena, V.; Malhotra, B. *Cur. App. Phy.* **2003,** *3*, 293. **DOI:** 10.1016/S1567-1739(02)00217-1
4. Inzelt, G.; Pineri, M.; Schultze, J. W.; Vorotyntsev, M. A. *Elect. Acta*. **2000,** *45*, 2403. **DOI:** 10.1016/S0013-4686(00)00329-7
5. Lu, W.; Fadeev, A. G.; Qi, B.; Mattes, B. R. *J. of The Electro. Soc.* **2004,** *151*, H33. **DOI:** 10.1149/1.1640635
6. Arulepp, M.; Permann, L.; Leis, J.; Perkson, A.; Rumma, K.; Jänes, A.; Lust, E. *J. of Pow. Sou.* **2004,** *133*, 320. **DOI:** 10.1016/j.jpowsour.2004.03.026
7. Yadav, R. S.; Singh, R. P.; Verma, P.; Tiwari, A.; Pandey, A. C; In Int. Nanomat.; John Wiley & Sons, Inc., **2012**. **DOI:**10.1002/9781118311974.ch6
8. Wang, Y.; Jing, X. *Poly. for Ad. Tech.* **2005,** *16*, 344. **DOI:** 10.1002/pat.589
9. Dhawan, S.; Singh, N.; Rodrigues, D. *Sci. and Tech. of Ad. Mat.* **2003,** *4*, 105. **DOI:** 10.1016/S1468-6996(02)00053-0
10. Mutiso, R. M.; Winey, K. I. *Prog. in Poly. Sci.* **2015,** *40*, 63. **DOI:** 10.1016/j.progpolymsci.2014.06.002
11. David, T.; Mathad, J. K.; Padmavathi, T.; Vanaja, A. *Polymer* **2014,** *55*, 5665. **DOI:** 10.1016/j.polymer.2014.09.007
12. Khairy, M. *Syn. Met.* **2014**, *189*, 34. **DOI:** 10.1016/j.synthmet.2013.12.022
13. Pang, H.; Xu, L.; Yan, D.-X.; Li, Z.-M. *Prog. in Poly. Sci.* **2014**, *39*, 1908. **DOI:** 10.1016/j.progpolymsci.2014.07.007
14. Singh, A. P.; Mishra, M.; Sambyal, P.; Gupta, B. K.; Singh, B. P.; Chandra, A.; Dhawan, S. K.. *J. of Mat. Chem. A*. **2014,** *2*, 3581. **DOI:** 10.1039/C3TA14212D
15. Soto-Oviedo, M. A.; AraÃºjo, O. A.; Faez, R.; Rezende, M. C.; De Paoli, M.-A. *Syn. Met.* **2006**,*156*, 1249. **DOI:** 10.1016/j.synthmet.2006.09.003
16. Singh, A. P.; S., A. K.; Amita Chandra; K. Dhawan, S. *Aip Adv.* **2011**, *1*, 022147. **DOI:** http://dx.doi.org/10.1063/1.3608052
17. Roy, R.; Bhattacharyya, A.; Sen, S. K.; Sen, S. *phy. sta. sol. (a)*. **1998**, *165*, 245. **DOI:** 10.1002/(SICI)1521-396X(199801)165:1<245::AID-PSSA245>3.0.CO;2-Y
18. Alperstein, D.; Narkis, M.; Zilberman, M.; Siegmann, A. *Poly. for Adv.Tech.* **1998**, *9*, 563. **DOI:** 10.1002/(SICI)1099-1581(199809)9:9<563::AID-PAT820>3.0.CO;2-4
19. Pud, A.; Ogurtsov, N.; Korzhenko, A.; Shapoval, G. *Prog. in Poly. Sci.* **2003**, *28*, 1701. **DOI:** 10.1016/j.progpolymsci.2003.08.001
20. Mav, I.; Zigon, M. *Syn. Met.* **2001 1**,*19*, 145. **DOI:** 10.1016/S0379-6779(00)01289-3
21. Kulkarni, M. V.; Viswanath, A. K.. *Eur. Poly. Jour.* **2004**, *40*, 379. **DOI:** 10.1016/j.eurpolymj.2003.10.007
22. Wazzan, A.; Ismail, M.; Abd El Ghaffar, M. *Int.J. of Poly. Ana. and Char.* **2005**, *10*, 57. **DOI:** 10.1080/10236660500345976
23. Kondawar, S. B.; Patil, P. T.; Agrawal, S. P. *Adv.Mat. Let.* **2014**, *5*. **DOI:** 10.5185/amlett.2014.amwc.1037
24. Adhikari, B.; Majumdar, S.; *Prog.in Poly. Sci.*, **2004**, *29*, 699. **DOI:** 10.1016/j.progpolymsci.2004.03.002
25. Sathiyanarayanan, S.; Dhawan, S.; Trivedi, D.; Balakrishnan, K. *Corr. Sci.* **1992**, 33, 1831. **DOI:** 10.1016/0010-938X(92)90187-8
26. Ramalingam, M.; Tiwari, A. *Intelligent Nanomaterials: Processes, Properties, and Applications*. **2012**, 801. **DOI:** 10.1002/9781118311974
27. Kumar, R.; Joon, S.; Singh, A. P.; Singh, B.; Dhawan, S. *Ame. Jou. of Poly. Sci.* **2015**, 5, 28. **DOI:** 10.5923/s.ajps.201501.04
28. Varshney, S.; Ohlan, A.; Singh, K.; Jain, V. K.; Dutta, V. P.; Dhawan, S. K. *Sci. of Adv. Mat.* **2013,** 5, 881. **DOI:** 10.1016/j.jallcom.2012.05.119
29. Li, L.; Chung, D. *Composites*. **1994**, 25, 215. **DOI:** 10.1016/0010-4361(94)90019-1
30. Thomassin, J.-M.; Jérôme, C.; Pardoen, T.; Bailly, C.; Huynen, I.; Detrembleur, C. *Mat. Sci. and Eng.: R: Rep.* **2013**,74, 211. **DOI:** 10.1016/j.mser.2013.06.001
31. Hino, T.; Namiki, T.; Kuramoto, N.; *Syn. Met.*, **2006**, 156, 1327. **DOI:** 10.1016/j.synthmet.2006.10.001
32. Varshney, S.; Singh, K.; Ohlan, A.; Jain, V. K.; Dutta, V. P.; Dhawan, S. K. *J. of All. and Com.* **2012**, 538, 107. **DOI:** 10.1016/j.jallcom.2012.05.119
33. Kulkarni, M. V.; Viswanath, A. K. *Sen. and Act. B: Chem.* **2005,** 107, 791. **DOI:** 10.1016/j.snb.2004.12.019
34. Klink, M. J.; Iwuoha, E.; Ebenso, E. E. *Int. J. Elec.. Sci*. **2012**, 7, 3031. **DOI:** http://www.electrochemsci.org/papers/vol7/7043031.pdf
35. Cataldo, F.; Maltese, P. *Eur. Poly. Jour.* **2002**, 38, 1791. **DOI:** 10.1016/S0014-3057(02)00070-8
36. Hwang, G.-W.; Wu, K.-Y.; Hua, M.-Y.; Lee, H.-T.; Chen, S.-A. *Synthetic Metals* **1998**, 92, 39. **DOI:** 10.1016/S0379-6779(98)80020-9

37. Stejskal, J.; OmastovÃ¡, M. r.; Fedorova, S.; ProkeÅ¡, J.; TrchovÃ¡, M. *Polymer* **2003**, 44, 1353.
DOI: 10.1016/S0032-3861(02)00906-0
38. Rao, P. S.; Subrahmanya, S.; Sathyanarayana, D. N. *Syn. Met.* **2002**, 128, 311.
DOI: 10.1016/S0379-6779(02)00016-4
39. Tripathi, P.; Prakash Patel, C. R.; Dixit, A.; Singh, A. P.; Kumar, P.; Shaz, M. A.; Srivastava, R.; Gupta, G.; Dhawan, S. K.; Gupta, B. K.; Srivastava, O. N. *Rsc Adv.* **2015**, 5, 19074.
DOI: 10.1039/c4ra17230b
40. Singh, A. P.; Mishra, M.; Hashim, D. P.; Narayanan, T.; Hahm, M. G.; Kumar, P.; Dwivedi, J.; Kedawat, G.; Gupta, A.; Singh, B. P. in Carbon **2015**, p 79.
DOI: 10.1016/j.carbon.2014.12.065
41. Reshi, H. A.; Singh, A. P.; Pillai, S.; Yadav, R. S.; Dhawan, S. K.; Shelke, V. *Journal of Materials Chemistry C*. **2014**.
DOI: 10.1039/c4tc02040e
42. Gupta, T. K.; Singh, B. P.; Singh, V. N.; Teotia, S.; Singh, A. P.; Elizabeth, I.; Dhakate, S. R.; Dhawan, S. K.; Mathur, R. B. *Journal of Materials Chemistry A* **2013**, 2, 4256.
DOI: 10.1039/c3ta14854h
43. Kumar, A.; Singh, A. P.; Kumari, S.; Dutta, P. K.; Sk, D.; Dhar, A. *Journal of Materials Chemistry A*. **2014.**
DOI: 10.1039/c4ta01655f

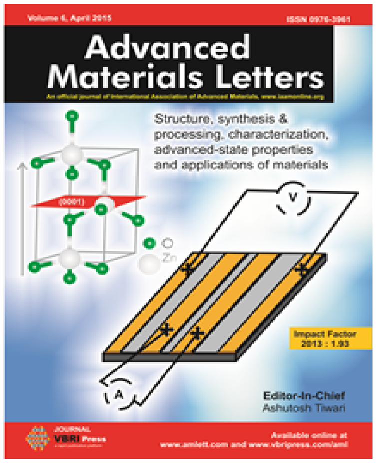

Supporting Information

Conductivity measurement of powder samples

The powder samples have been compressed by hydraulic press to get rectangular pallets and conductivity is measured by the same technique using Keithley programmable current source (model 6221).

Sample name	**Carbon fiber (wt. %)**	**Novolac resin (wt. %)**	**Electrical conductivity (S/cm)**
PoA	0	0	0.94×10^{-3}
PoACF	20	0	2.43×10^{-1}
PoACF5 powder	20	5	0.63×10^{-1}
PoACF15 powder	20	15	0.41×10^{-1}
PoACF25 powder	20	25	0.11×10^{-2}
PoACF5 sheet	20	5	0.95×10^{-1}
PoACF15 sheet	20	15	0.64×10^{-1}
PoACF25 sheet	20	25	0.28×10^{-2}

Instrument for EMI shielding measurement of PoACF sheets

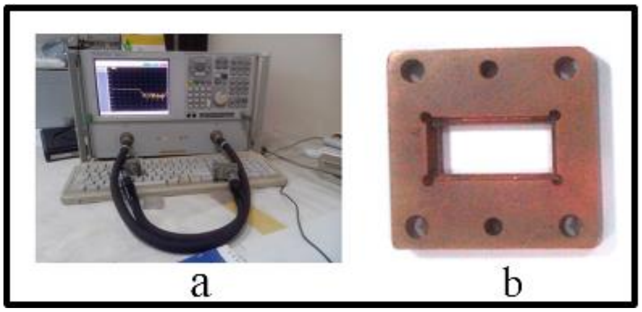

Fig. S 1. Photograph of Vector Network analyzer (a) for measuring scattering parameters and (b) shows the sample holder.